HIGHLIGHT OF THE MONTH

Orbital Functionals in Density Functional Theory: The Optimized Effective Potential Method

T. Grabo, E.K.U. Gross and M. Lüders

Institut für Theoretische Physik, Universität Würzburg,

Am Hubland, D-97074 Würzburg, Germany

The success of density functional theory hinges on the availability of good approximations for the total-energy functional. In this article we review a particular approach to the construction of approximations involving explicitly orbital-dependent functionals. The advantages of this approach over the conventional Kohn-Sham scheme are highlighted and numerical results are presented for atoms, molecules and solids.

1 Introduction: What is the optimized effective potential?

The optimized effective potential (OEP) is not a new development. In fact, its discovery [1] preceeds the development of modern density functional theory. In present-day language, the *exact* OEP should be called the *exact* Kohn-Sham (KS) potential. When it comes to approximations, however, the OEP representation of the KS potential allows for the construction of more accurate functionals than the conventional local density (LDA) or generalized gradient (GGA) approximations. In order to understand the nature of the OEP we first briefly review the basics of density functional theory (DFT).

Modern DFT is based on the celebrated theorem of Hohenberg and Kohn (HK) [2] which may be summarized by the following three statements:

1. The ground-state density ρ uniquely determines the external potential $V = V[\rho]$ as well as the ground-state wave function $\Psi[\rho]$. As a consequence, any observable of a static many-particle system is a functional of its ground state density.

2. If $\hat{T}$ denotes the kinetic energy operator of the particles and $\hat{W}_{\mathrm{Clb}}$ their mutual Coulomb interaction, the total-energy functional

$$E_{v_0}[\rho] := < \Psi[\rho]|\hat{T} + \hat{W}_{\mathrm{Clb}} + \hat{V}_0|\Psi[\rho] > \tag{1}$$

of a particular physical system characterized by the external potential V_0 is equal to the exact ground-state energy E_0 if and only if the exact ground-state density ρ_0 is inserted. For all other densities $\rho \neq \rho_0$ the inequality

$$E_0 < E_{v_0}[\rho] \tag{2}$$

holds. Consequently, the exact ground-state density ρ_0 and the exact ground-state energy E_0 can be determined by solving the Euler-Lagrange equation

$$\frac{\delta}{\delta\rho(\mathbf{r})}E_{v_0}[\rho] = 0. \tag{3}$$

3. The functional

$$F[\rho] := < \Psi[\rho]|\hat{T} + \hat{W}_{\mathrm{Clb}}|\Psi[\rho] > \tag{4}$$

is universal in the sense that it is independent of the external potential V_0 of the particular system considered, i.e. it is of the same functional form for all systems with a fixed particle-particle interaction ($\hat{W}_{\mathrm{Clb}}$ in our case).

The proof of the HK theorem does not depend on the particular form of the particle-particle interaction. It is valid for *any* given particle-particle interaction $\hat{W}$, in particular also for $\hat{W} \equiv 0$, i.e. for non-interacting systems described by Hamiltonians of the form $\hat{H}_S = \hat{T} + \hat{V}_S$. Hence the potential $V_S(\mathbf{r})$ is uniquely determined by the ground-state density:

$$V_S(\mathbf{r}) = V_S[\rho](\mathbf{r}). \tag{5}$$

As a consequence, all single-particle orbitals satisfying the Schrödinger equation (atomic units are used throughout)

$$\left(-\frac{\nabla^2}{2} + V_S[\rho](\mathbf{r})\right)\varphi_j(\mathbf{r}) = \varepsilon_j\varphi_j(\mathbf{r}) \tag{6}$$

are functionals of the density as well:

$$\varphi_j(\mathbf{r}) = \varphi_j[\rho](\mathbf{r}). \tag{7}$$

The HK total-energy functional of non-interacting particles is given by

$$E_S[\rho] = T_S[\rho] + \int \mathrm{d}^3r\, \rho(\mathbf{r})V_S(\mathbf{r}) \tag{8}$$

where $T_S[\rho]$ is the kinetic-energy functional of non-interacting particles:

$$T_S[\rho] = \sum_{\substack{i=1 \\ \text{lowest } \varepsilon_i}}^{N} \int r m d^3 r\, \varphi_i^*[\rho](\mathbf{r}) \left(-\frac{\nabla^2}{2}\right) \varphi_i[\rho](\mathbf{r}). \tag{9}$$

We emphasize that the quantity (9) really represents a *functional of the density:* Functional means that we can assign a unique number $T_S[\rho]$ to any function $\rho(\mathbf{r})$. This is done by first calculating that very potential $V_S(\mathbf{r})$ which uniquely corresponds to $\rho(\mathbf{r})$. Several numerical schemes have been devised to achieve this task [3, 4, 5, 6, 7, 8]. Then we take this potential, solve the Schrödinger equation (6) with it to obtain a set of orbitals $\{\varphi_j(\mathbf{r})\}$ and use those to calculate the number T_S by evaluating the right-hand side of Eq. (9). As a matter of fact, by the same chain of arguments, *any orbital functional is an (implicit) functional of the density,* provided the orbitals come from a local, i.e. multiplicative potential.

Returning to the *interacting* system of interest we now define the so-called exchange-correlation (xc) energy functional by

$$E_{\mathrm{xc}}[\rho] := F[\rho] - \frac{1}{2} \int \mathrm{d}^3 r \int \mathrm{d}^3 r' \, \frac{\rho(\mathbf{r})\rho(\mathbf{r}')}{|\mathbf{r} - \mathbf{r}'|} - T_{\mathrm{S}}[\rho]. \tag{10}$$

The HK total-energy functional (1) can then be written as

$$E_{v_0}[\rho] = T_{\mathrm{S}}[\rho] + \int \mathrm{d}^3 r\, \rho(\mathbf{r}) v_0(\mathbf{r}) + \frac{1}{2} \int \mathrm{d}^3 r \int \mathrm{d}^3 r' \, \frac{\rho(\mathbf{r})\rho(\mathbf{r}')}{|\mathbf{r} - \mathbf{r}'|} + E_{\mathrm{xc}}[\rho]. \tag{11}$$

In historical retrospective we may identify three generations of density functional schemes which may be classified according to the level of approximations used for the universal functionals $T_S[\rho]$ and $E_{\mathrm{xc}}[\rho]$.

In what we call the *first generation of DFT, explicitly* density-dependent functionals are used to approximate both $T_S[\rho]$ and $E_{\mathrm{xc}}[\rho]$. For example, the simplest and historically first approximation of this kind is the Thomas-Fermi model, where $E_{\mathrm{xc}}[\rho]$ is neglected completely and $T_S[\rho]$ is approximated by an LDA yielding

$$E_{v_0}^{\mathrm{TF}}[\rho] = \frac{3}{10} \left(3\pi^2\right)^{2/3} \int \mathrm{d}^3 r\, \rho(\mathbf{r})^{5/3} + \int \mathrm{d}^3 r\, v_0(\mathbf{r})\rho(\mathbf{r}) + \frac{1}{2} \int \mathrm{d}^3 r \int \mathrm{d}^3 r' \, \frac{\rho(\mathbf{r})\rho(\mathbf{r}')}{|\mathbf{r} - \mathbf{r}'|} \tag{12}$$

as approximate expression for the total-energy functional. For functionals of this type the HK variational principle (3) can be used directly, leading to variational equations of the Thomas-Fermi type. As these equations only contain one basic variable, namely the density $\rho(\mathbf{r})$ of the system, they are readily solved numerically. The results obtained in this way, however, are generally of moderate quality.

The *second generation* of DFT employs the *exact* functional (9) for the non-interacting kinetic energy and an approximate density functional for the xc energy:

$$E_{v_0}^{\mathrm{KS}}[\rho] = T_{\mathrm{S}}^{\mathrm{exact}}[\rho] + \int \mathrm{d}^3 r\, v_0(\mathbf{r})\rho(\mathbf{r}) + \frac{1}{2} \int \mathrm{d}^3 r \int \mathrm{d}^3 r' \, \frac{\rho(\mathbf{r})\rho(\mathbf{r}')}{|\mathbf{r} - \mathbf{r}'|} + E_{\mathrm{xc}}[\rho]. \tag{13}$$

This total-energy expression leads to the conventional Kohn-Sham version of DFT [9]. The HK variational principle (3) applied to (13) leads to a unique single-particle potential (which is commonly referred to as KS potential)

$$V_S[\rho](\mathbf{r}) = V_0(\mathbf{r}) + \int \mathrm{d}^3 r' \, \frac{\rho(\mathbf{r}')}{|\mathbf{r} - \mathbf{r}'|} + \frac{\delta E_{\mathrm{xc}}[\rho]}{\delta \rho(\mathbf{r})} \tag{14}$$

such that the orbitals resulting from (6) with the potential (14) reproduce the density of the interacting system of interest.

Finally, in the *third generation, which is the OEP version of DFT,* one employs in addition to the *exact* expression for T_S also the *exact* expression for the exchange energy given by

$$E_{\mathrm{x}}^{\mathrm{exact}}[\rho] = -\frac{1}{2} \sum_{\sigma=\uparrow,\downarrow} \sum_{j,k=1}^{N_\sigma} \int \mathrm{d}^3 r \int \mathrm{d}^3 r' \, \frac{\varphi_{j\sigma}^*(\mathbf{r}) \varphi_{k\sigma}^*(\mathbf{r}') \varphi_{k\sigma}(\mathbf{r}) \varphi_{j\sigma}(\mathbf{r}')}{|\mathbf{r} - \mathbf{r}'|}. \tag{15}$$

Only the correlation part of $E_{\mathrm{xc}}[\rho]$ needs to be approximated in this approach. In contrast to the conventional second-generation KS-scheme, the third generation allows for the treatment of explicitly orbital-dependent functionals for the correlation energy E_{c} as well, giving more flexibility in the construction of such approximations.

The central equation in the OEP version of DFT is still the KS equation (6) and the xc potential is still given by the functional derivative

$$V_{\mathrm{xc}}^{\mathrm{OEP}}(\mathbf{r}) = \frac{\delta E_{\mathrm{xc}}}{\delta \rho(\mathbf{r})}. \tag{16}$$

The difference between the second and third generations lies in the level of approximation to the xc-energy. As a consequence of the orbital dependence of E_{xc} in the third generation of DFT the calculation of $V_{\mathrm{xc}}[\rho](\mathbf{r})$ from Eq. (16) is somewhat more complicated. A detailed derivation will be given in the following section for the spin-dependent version of DFT. The result is an integral equation determining the xc potential. This integral equation, known as the optimized effective potential equation, is very hard to solve numerically. To avoid a full-scale numerical solution, Krieger, Li and Iafrate [10, 11] have devised a semi-analytical scheme for solving the OEP integral equation approximately. This scheme is described in the following section as well. Finally a selection of numerical results for atoms, molecules and solids will be presented in the last section.

We mention that a time-dependent generalization of the OEP has recently been developed [12] to deal with explicitly time-dependent situations such as atoms in strong laser pulses [13]. In the linear-response regime this method has led to a rather successful procedure [14] to calculate excitation energies from the poles of the frequency-dependent density response. Time-dependent applications of this kind will not be discussed in the present article. The interested reader is referred to a recent review of time-dependent DFT [15].

2 Basic formalism of the OEP and KLI methods

We are going to derive the OEP equations for the spin-dependent version of DFT [16, 17], where the basic variables are the spin-up and spin-down densities $\rho_\uparrow(\mathbf{r})$ and $\rho_\downarrow(\mathbf{r})$, respectively. The latter are obtained by self-consistently solving the KS equations

$$\left(-\frac{\nabla^2}{2} + V_{S\sigma}[\rho_\uparrow, \rho_\downarrow](\mathbf{r})\right) \varphi_{j\sigma}(\mathbf{r}) = \varepsilon_{j\sigma}\varphi_{j\sigma}(\mathbf{r}) \qquad j = 1, \ldots, N_\sigma \qquad \sigma = \uparrow, \downarrow \qquad (17)$$

where

$$\rho_\sigma(\mathbf{r}) = \sum_{i=1}^{N_\sigma} |\varphi_{i\sigma}(\mathbf{r})|^2. \tag{18}$$

The Kohn-Sham potentials $V_{S\sigma}(\mathbf{r})$ may be written in the usual way as

$$V_{S\sigma}(\mathbf{r}) = v_0(\mathbf{r}) + \int \mathrm{d}^3r' \, \frac{\rho(\mathbf{r}')}{|\mathbf{r} - \mathbf{r}'|} + V_{\mathrm{xc}\sigma}(\mathbf{r}), \tag{19}$$

$$\rho(\mathbf{r}) = \sum_{\sigma=\uparrow,\downarrow} \rho_\sigma(\mathbf{r}) \tag{20}$$

where

$$V_{\mathrm{xc}\sigma}(\mathbf{r}) := \frac{\delta E_{\mathrm{xc}}[\rho_\uparrow, \rho_\downarrow]}{\delta\rho_\sigma(\mathbf{r})}. \tag{21}$$

The starting point of the OEP method is the total-energy functional

$$
\begin{aligned}
E_{v_0}^{\mathrm{OEP}}[\rho_\uparrow, \rho_\downarrow] &= \sum_{\sigma=\uparrow,\downarrow} \sum_{i=1}^{N_\sigma} \int \mathrm{d}^3r \, \varphi_{i\sigma}^*(\mathbf{r}) \left(-\frac{1}{2}\nabla^2\right) \varphi_{i\sigma}(\mathbf{r}) \\
&+ \int \mathrm{d}^3r \, v_0(\mathbf{r})\rho(\mathbf{r}) \\
&+ \frac{1}{2} \int \mathrm{d}^3r \int \mathrm{d}^3r' \, \frac{\rho(\mathbf{r})\rho(\mathbf{r}')}{|\mathbf{r} - \mathbf{r}'|} \\
&+ E_{\mathrm{xc}}^{\mathrm{OEP}}[\{\varphi_{j\tau}\}]
\end{aligned}
\tag{22}
$$

where, in contrast to ordinary spin DFT, the xc energy is an *explicit* (approximate) functional of spin orbitals and therefore only an *implicit* functional of the spin densities $\rho_\uparrow$ and $\rho_\downarrow$. In order to calculate the xc potentials from Eq. (21) we use the chain rule for functional derivatives to obtain

$$
\begin{aligned}
V_{\mathrm{xc}\sigma}^{\mathrm{OEP}}(\mathbf{r}) &= \frac{\delta E_{\mathrm{xc}}^{\mathrm{OEP}}[\{\varphi_{j\tau}\}]}{\delta\rho_\sigma(\mathbf{r})} \\
&= \sum_{\alpha=\uparrow,\downarrow} \sum_{i=1}^{N_\alpha} \int \mathrm{d}^3r' \, \frac{\delta E_{\mathrm{xc}}^{\mathrm{OEP}}[\{\varphi_{j\tau}\}]}{\delta\varphi_{i\alpha}(\mathbf{r}')} \frac{\delta\varphi_{i\alpha}(\mathbf{r}')}{\delta\rho_\sigma(\mathbf{r})} + c.c.
\end{aligned}
\tag{23}
$$

and, by applying the functional chain rule once more,

$$V_{\mathrm{xc}\sigma}^{\mathrm{OEP}}(\mathbf{r}) = \sum_{\alpha=\uparrow,\downarrow} \sum_{\beta=\uparrow,\downarrow} \sum_{i=1}^{N_\alpha} \int \mathrm{d}^3r' \int \mathrm{d}^3r'' \left(\frac{\delta E_{\mathrm{xc}}^{\mathrm{OEP}}[\{\varphi_{j\tau}\}]}{\delta\varphi_{i\alpha}(\mathbf{r}')} \frac{\delta\varphi_{i\alpha}(\mathbf{r}')}{\delta V_{S\beta}(\mathbf{r}'')} + c.c.\right) \frac{\delta V_{S\beta}(\mathbf{r}'')}{\delta\rho_\sigma(\mathbf{r})}. \tag{24}$$

The last term on the right-hand side is readily identified with the inverse $\chi_S^{-1}(\mathbf{r}, \mathbf{r}')$ of the density response function of a system of non-interacting particles

$$\chi_{S\alpha,\beta}(\mathbf{r}, \mathbf{r}') := \frac{\delta \rho_\alpha(\mathbf{r})}{\delta V_{S\beta}(\mathbf{r}')}. \tag{25}$$

This quantity is diagonal with respect to the spin variables so that Eq. (24) reduces to

$$V_{\mathrm{xc}\sigma}^{\mathrm{OEP}}(\mathbf{r}) = \sum_{\alpha=\uparrow,\downarrow} \sum_{i=1}^{N_\alpha} \int \mathrm{d}^3 r' \int \mathrm{d}^3 r'' \left(\frac{\delta E_{\mathrm{xc}}^{\mathrm{OEP}}[\{\varphi_{j\tau}\}]}{\delta \varphi_{i\alpha}(\mathbf{r}')} \frac{\delta \varphi_{i\alpha}(\mathbf{r}')}{\delta V_{S\sigma}(\mathbf{r}'')} + c.c. \right) \chi_{S\sigma}^{-1}(\mathbf{r}'', \mathbf{r}). \tag{26}$$

Acting with the response operator (25) on both sides of Eq. (26) one obtains

$$\int \mathrm{d}^3 r' \, V_{\mathrm{xc}\sigma}^{\mathrm{OEP}}(\mathbf{r}') \chi_{S\sigma}(\mathbf{r}', \mathbf{r}) = \sum_{\alpha=\uparrow,\downarrow} \sum_{i=1}^{N_\alpha} \int \mathrm{d}^3 r' \, \frac{\delta E_{\mathrm{xc}}^{\mathrm{OEP}}[\{\varphi_{j\tau}\}]}{\delta \varphi_{i\alpha}(\mathbf{r}')} \frac{\delta \varphi_{i\alpha}(\mathbf{r}')}{\delta V_{S\sigma}(\mathbf{r})} + c.c.. \tag{27}$$

Finally, the second functional derivative on the right-hand side of Eq. (27) is calculated using first-order perturbation theory. This yields

$$\frac{\delta \varphi_{i\alpha}(\mathbf{r}')}{\delta V_{S\sigma}(\mathbf{r})} = \delta_{\alpha,\sigma} \sum_{\substack{k=1 \\ k\neq i}}^{\infty} \frac{\varphi_{k\sigma}(\mathbf{r}')\varphi_{k\sigma}^*(\mathbf{r})}{\varepsilon_{i\sigma} - \varepsilon_{k\sigma}} \varphi_{i\sigma}(\mathbf{r}). \tag{28}$$

Using this equation, the response function

$$\chi_{S\alpha,\beta}(\mathbf{r}, \mathbf{r}') = \frac{\delta}{\delta V_{S\beta}(\mathbf{r}')} \left(\sum_{i=1}^{N_\alpha} \varphi_{i\alpha}^*(\mathbf{r})\varphi_{i\alpha}(\mathbf{r}) \right) \tag{29}$$

is readily expressed in terms of the orbitals as

$$\chi_{S\sigma}(\mathbf{r}, \mathbf{r}') = \sum_{i=1}^{N_\sigma} \sum_{\substack{k=1 \\ k\neq i}}^{\infty} \frac{\varphi_{i\sigma}^*(\mathbf{r})\varphi_{k\sigma}(\mathbf{r})\varphi_{k\sigma}^*(\mathbf{r}')\varphi_{i\sigma}(\mathbf{r}')}{\varepsilon_{i\sigma} - \varepsilon_{k\sigma}} + c.c.. \tag{30}$$

Inserting (28) and (30) in Eq. (27), we obtain the standard form of the OEP integral equation:

$$\sum_{i=1}^{N_\sigma} \int \mathrm{d}^3 r' \left(V_{\mathrm{xc}\sigma}^{\mathrm{OEP}}(\mathbf{r}') - u_{\mathrm{xc}i\sigma}(\mathbf{r}') \right) G_{Si\sigma}(\mathbf{r}', \mathbf{r}) \, \varphi_{i\sigma}(\mathbf{r})\varphi_{i\sigma}^*(\mathbf{r}') + c.c. = 0 \tag{31}$$

where

$$u_{\mathrm{xc}i\sigma}(\mathbf{r}) := \frac{1}{\varphi_{i\sigma}^*(\mathbf{r})} \frac{\delta E_{\mathrm{xc}}^{\mathrm{OEP}}[\{\varphi_{j\tau}\}]}{\delta \varphi_{i\sigma}(\mathbf{r})} \tag{32}$$

and

$$G_{Si\sigma}(\mathbf{r}, \mathbf{r}') := \sum_{\substack{k=1 \\ k\neq i}}^{\infty} \frac{\varphi_{k\sigma}(\mathbf{r})\varphi_{k\sigma}^*(\mathbf{r}')}{\varepsilon_{i\sigma} - \varepsilon_{k\sigma}}. \tag{33}$$

The derivation of the OEP integral equation (31) described here was first given by Görling and Levy [18]. It is important to note that the same expression results [1, 19, 10, 20] if one

demands that the local one-particle potential appearing in Eq. (17) be the *optimized* one yielding orbitals minimizing the total-energy functional (22), i.e. that

$$\left. \frac{\delta E_{v_0}^{OEP}}{\delta V_{S\sigma}(\mathbf{r})} \right|_{V_S = V^{OEP}} = 0. \tag{34}$$

This equation is the historical origin [1] of the name *optimized effective potential*.

In order to use the OEP, one has to solve the OEP integral equation (31) for the xc potential $V_{xc\sigma}^{OEP}$ in each iterative step of the KS self-consistency cycle. This is a rather demanding task and has been achieved so far only for systems of high symmetry such as spherical atoms [19, 10, 21] and for solids within the linear muffin tin orbitals atomic sphere approximation [22, 23, 24].

To avoid the full-scale numerical solution of the OEP integral equation Krieger, Li and Iafrate (KLI) [11] suggested a semi-analytical approximation. It can be derived by replacing the energy denominators in the Green's function type quantity (33) by an average energy difference independent of i and k:

$$G_{si\sigma}(\mathbf{r}, \mathbf{r}') \approx \frac{1}{\triangle\epsilon}\left(\delta(\mathbf{r} - \mathbf{r}') - \varphi_{i\sigma}(\mathbf{r})\varphi_{i\sigma}^*(\mathbf{r}')\right). \tag{35}$$

Substituting this into the integral equation (31) and performing some algebra one arrives at the equation

$$V_{xc\sigma}^{KLI}(\mathbf{r}) = \frac{1}{\rho_\sigma(\mathbf{r})} \sum_{i=1}^{N_\sigma} |\varphi_{i\sigma}(\mathbf{r})|^2 \left[U_{xci\sigma}(\mathbf{r}) + \left(\bar{V}_{xci\sigma} - \bar{U}_{xci\sigma}\right)\right] \tag{36}$$

where $U_{xci\sigma}(\mathbf{r}) = \frac{1}{2}(u_{xci\sigma}(\mathbf{r}) + u_{xci\sigma}^*(\mathbf{r}))$ and $\bar{U}_{xcj\sigma}$ denotes the average value of $U_{xcj\sigma}(\mathbf{r})$ taken over the density of the $j\sigma$ orbital, i.e.

$$\bar{U}_{xcj\sigma} = \int \mathrm{d}^3r \, |\varphi_{j\sigma}(\mathbf{r})|^2 U_{xcj\sigma}(\mathbf{r}) \tag{37}$$

and similarly for $\bar{V}_{xci\sigma}$. In contrast to the exact integral equation (31) the KLI equation (36) can be solved explicitly for $V_{xc\sigma}$ by multiplication with $|\varphi_{i\sigma}(\mathbf{r})|^2$ and subsequent integration. This leads to an $(N_\sigma - 1) \times (N_\sigma - 1)$ system of linear equations for the unknown constants $\left(\bar{V}_{xci\sigma} - \bar{U}_{xci\sigma}\right)$:

$$\sum_{i=1}^{N_\sigma - 1} \left(\delta_{ji} - M_{ji\sigma}\right)\left(\bar{V}_{xci\sigma} - \bar{U}_{xci\sigma}\right) = \bar{V}_{xcj\sigma}^S - \bar{U}_{xcj\sigma} \qquad j = 1, \ldots, N_\sigma - 1 \tag{38}$$

with

$$M_{ji\sigma} := \int d^3r \, \frac{|\varphi_{j\sigma}(\mathbf{r})|^2 |\varphi_{i\sigma}(\mathbf{r})|^2}{\rho_\sigma(\mathbf{r})} \tag{39}$$

and

$$\bar{V}_{xcj\sigma}^S(\mathbf{r}) := \int \mathrm{d}^3r \, \frac{|\varphi_{j\sigma}(\mathbf{r})|^2}{\rho_\sigma(\mathbf{r})} \sum_{i=1}^{N} |\varphi_{i\sigma}(\mathbf{r})|^2 U_{xci\sigma}(\mathbf{r}). \tag{40}$$

It is an important property of the KLI approximation that it is exact for two-particle systems, where one has only one electron per spin projection. In this case, the OEP integral equation (31) may be solved exactly to yield (36).

7

At first sight, the KLI approximation (35) might appear rather crude. The final result (36) for the KLI potential, however, can also be understood [11] as a well-defined mean-field approximation. Explicit calculations on atoms performed in the x-only limit [25] show that the KLI-approximation yields excellent results with, e.g., ground-state energies differing only by a few ppm from the much more time-consuming exact solutions of the full integral equation (31). We will give numerical examples in the next section.

To conclude this section we describe (without proof) some exact properties of the OEP method and the KLI approximation.

1. **Asymptotics**

   For finite systems, both the full OEP and the KLI potential fall of as $-1/r$ for $r \to \infty$ [10] if the exact expression (15) for the exchange-energy functional is employed. The asymptotic behaviour of the correlation potential is equal to that of the function $u_{c,\mathrm{max}\sigma}(\mathbf{r})$ corresponding to the highest occupied orbital.

2. **Freedom of self-interaction**

   If the employed xc-energy functional cancels the self-interaction of the Hartree term, this property is preserved by the KLI approximation. Thus x-only OEP and x-only KLI schemes are self-interaction free. It has to be noted, however, that the inclusion of an LDA-correlation-energy functional might introduce a self-interaction error again.

3. **Derivative discontinuities**

   An important property of the *exact* xc potential is that it exhibits discontinuities as a function of particle number N at integer values of N. This has important consequences for the values of band gaps in insulators and semi-conductors (for a detailed description see e.g. [26]): The correct value E^g of the gap is obtained by adding the discontinuity Δ_{xc} of the xc potential to the KS gap, i.e. , $E^g = E^g_{\mathrm{KS}} + \Delta_{\mathrm{xc}}$. Neither the LDA nor the GGAs reproduce this discontinuity. To date, the OEP and the KLI potential are the only known approximations of $V_{\mathrm{xc}}(\mathbf{r})$ that reproduce this discontinuity [10].

3   Selected Results

3.1   Atomic and molecular systems

We begin with a comparison of x-only results. In an x-only world, the OEP represents the *exact* KS potential of DFT and can therefore serve as a standard to compare approximations with. In Table 1 we show as a typical example various results for the argon atom obtained with different x-only methods. Besides the exact OEP and KLI methods described above, we also list results from conventional KS-DFT obtained with the x-energy-functional approximations due to Becke (B88) [27], Perdew and Wang (PW91) [28] and from the well-known x-only LDA approximation. The KLI results given in the second column of Table 1 clearly demonstrate the high quality of the KLI approximation as all results differ only

Table 1: *Various self-consistently calculated x-only results for the Ar atom. All values in atomic units.*

	OEP	KLI	B88	xPW91	xLDA
E_{TOT}	-526.8122	-526.8105	-526.7998	-526.7710	-524.5174
ε_{1s}	-114.4524	-114.42789	-114.1890	-114.1887	-113.7159
ε_{2s}	-11.1534	-11.1820	-10.7911	-10.7932	-10.7299
ε_{2p}	-8.7339	-8.7911	-8.4107	-8.4141	-8.3782
ε_{3s}	-1.0993	-1.0942	-0.8459	-0.8481	-0.8328
ε_{3p}	-0.5908	-0.5893	-0.3418	-0.3441	-0.3338
ε_{4s}	-0.1607	-0.1616	-0.0106	-0.0122	-0.0014
$<r^2>$	1.4465	1.4467	1.4791	1.4876	1.4889
$<r^{-1}>$	3.8736	3.8738	3.8731	3.8729	3.8648
$\rho(0)$	3839.8	3832.6	3847.3	3847.0	3818.7

slightly from the exact OEP ones. For all standard DFT methods, the disagreement is much more pronounced, especially for the highest occupied orbital energies and *even more so for the unoccupied ones.* The reason for this may be seen from the plots of the x-potentials shown in Figures 1 and 2: The KLI potential is much closer to the exact OEP, reproducing the so-called inter-shell peaks, which are missing in the conventional KS approximations, and furthermore the correct $-1/r$ decay of $V_{\mathrm{x}}(\mathbf{r})$ for large r. This latter property is clearly visible from the plot in Figure 2, where we show $-V_{\mathrm{x}}(\mathbf{r})$ on a logarithmic scale. None of the standard KS potentials decays in a straight line with the proper slope as the OEP and KLI potentials do.

It has been shown [20, 32, 33] that the most suitable correlation-energy functional to be included into the KLI scheme is the one developed by Colle and Salvetti (CS) [34, 35]. It is given by

$$
\begin{aligned}
E_{\mathrm{c}}^{\mathrm{CS}}[\{\varphi_{i\sigma}\}] &= -ab \int \mathrm{d}^3 r \; \gamma(\mathbf{r})\xi(\mathbf{r}) \Bigg[\sum_\sigma \rho_\sigma(\mathbf{r}) \sum_i |\nabla\varphi_{i\sigma}(\mathbf{r})|^2 \; - \; \frac{1}{4}|\nabla\rho(\mathbf{r})|^2 \\
&\quad - \frac{1}{4}\sum_\sigma \rho_\sigma(\mathbf{r})\triangle\rho_\sigma(\mathbf{r}) \; + \; \frac{1}{4}\rho(\mathbf{r})\triangle\rho(\mathbf{r}) \Bigg] - a \int \mathrm{d}^3 r \; \gamma(\mathbf{r})\frac{\rho(\mathbf{r})}{\eta(\mathbf{r})},
\end{aligned} \qquad (41)
$$

where

$$
\gamma(\mathbf{r}) = 4\,\frac{\rho_\uparrow(\mathbf{r})\rho_\downarrow(\mathbf{r})}{\rho(\mathbf{r})^2}, \qquad (42)
$$

$$
\eta(\mathbf{r}) = 1 + d\rho(\mathbf{r})^{-\frac{1}{3}}, \qquad (43)
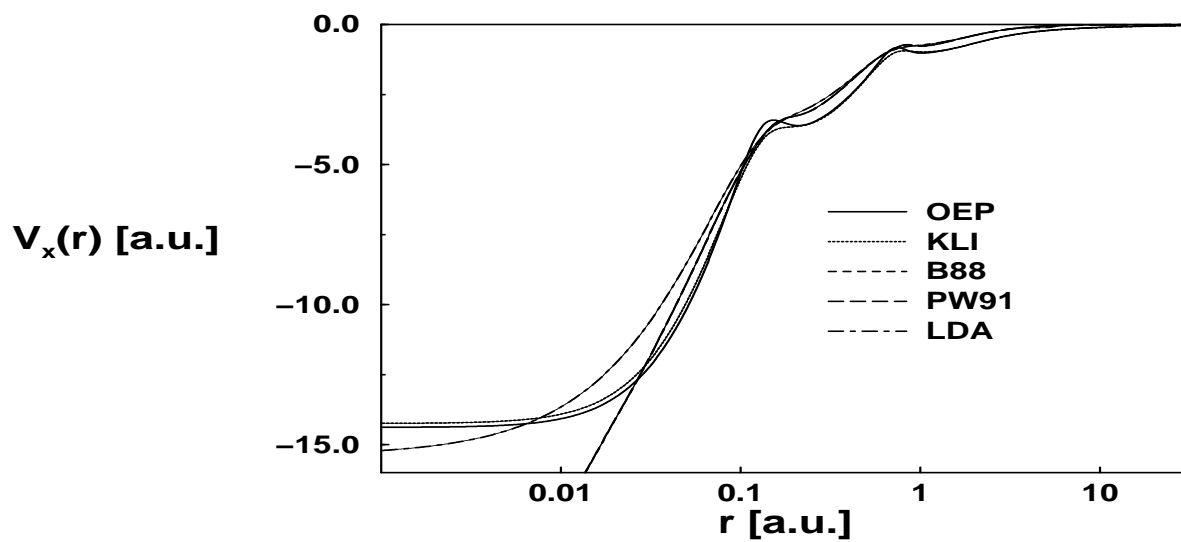$$

9

Figure 1: *Exchange potentials $V_x(\mathbf{r})$ of the Ar atom from various self-consistent calculations.*
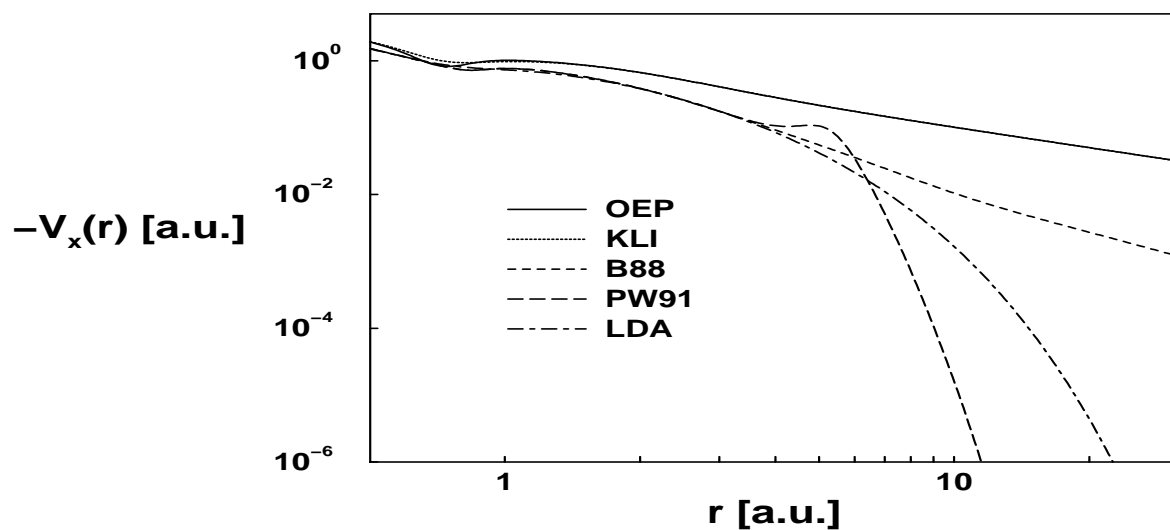

Figure 2: *Exchange potentials $-V_x(\mathbf{r})$ of the Ar atom from various self-consistent calculations in the valence region.*

Table 2: *Total absolute ground-state energies for first-row atoms from various self-consistent calculations [20]. Quantum chemistry (QC) values from [29]. $\bar{\triangle}$ denotes the mean absolute deviation from the exact non-relativistic values [30]. All numbers in atomic units.*

	KLICS	LDA	BLYP	PW91	QC	exact
He	2.9033	2.8348	2.9071	2.9000	2.9049	2.9037
Li	7.4829	7.3440	7.4827	7.4742	7.4743	7.4781
Be	14.6651	14.4472	14.6615	14.6479	14.6657	14.6674
B	24.6564	24.3536	24.6458	24.6299	24.6515	24.6539
C	37.8490	37.4700	37.8430	37.8265	37.8421	37.8450
N	54.5905	54.1368	54.5932	54.5787	54.5854	54.5893
O	75.0717	74.5274	75.0786	75.0543	75.0613	75.067
F	99.7302	99.1142	99.7581	99.7316	99.7268	99.734
Ne	128.9202	128.2335	128.9730	128.9466	128.9277	128.939
$\bar{\triangle}$	0.0047	0.3795	0.0108	0.0114	0.0045	

$$\xi(\mathbf{r}) \;\; = \;\; \frac{\rho(\mathbf{r})^{-\frac{5}{3}} e^{-c\rho(\mathbf{r})^{-\frac{1}{3}}}}{\eta(\mathbf{r})}. \tag{44}$$

The constants a, b, c and d are given by $a = 0.04918$, $b = 0.132$, $c = 0.2533$, $d = 0.349$.

In Table 2 we compare total ground-state energies of first-row atoms calculated self-consistently with various approximations. The first column, headed KLICS, shows the results from the KLI method employing the exact exchange energy functional (15) plus the CS-correlation energy functional while the next columns show conventional KS results obtained with the x-energy functional due to Becke [27] combined with the c-energy functional from Lee, Yang and Parr [36], denoted as BLYP, and from the generalized gradient approximation due to Perdew and Wang [28], referred to as PW91. The quantum chemistry values, headed QC, are based on configuration interaction calculations [29]. The exact non-relativistic energies, i.e. the experimental values with relativistic effects subtracted, have been taken from [30]. The mean absolute deviations of the calculated from the exact values, denoted by $\bar{\triangle}$, are about the same for the KLICS and QC approaches, while they are about twice as high for the GGAs and about a factor of 80 higher in the LDA. We emphasize that the numerical effort involved in the KLICS scheme for atoms is only slightly higher than in the LDA and GGA schemes. Apart from total energies, the highest occupied orbital energies, which should be equal to the exact ionization potential in an exact implementation of DFT, are much closer to the experimental ionization potentials in the KLICS scheme than in the conventional KS approaches. This is shown in Table 3: All the conventional KS-calculations

Table 3: *Ionization potentials of neutral atoms, calculated from the highest occupied orbital energies [20].* $\bar{\triangle}$ *denotes the mean absolute deviation from the experimental values, taken from [31]. All values in atomic units.*

	KLICS	LDA	BLYP	PW91	experiment
He	0.945	0.570	0.585	0.583	0.903
Li	0.200	0.116	0.111	0.119	0.198
Be	0.329	0.206	0.201	0.207	0.343
B	0.328	0.151	0.143	0.149	0.305
C	0.448	0.228	0.218	0.226	0.414
N	0.579	0.309	0.297	0.308	0.534
O	0.559	0.272	0.266	0.267	0.500
F	0.714	0.384	0.376	0.379	0.640
Ne	0.884	0.498	0.491	0.494	0.792
Na	0.189	0.113	0.106	0.113	0.189
Mg	0.273	0.175	0.168	0.174	0.281
Al	0.222	0.111	0.102	0.112	0.220
Si	0.306	0.170	0.160	0.171	0.300
P	0.399	0.231	0.219	0.233	0.385
S	0.404	0.228	0.219	0.222	0.381
Cl	0.506	0.305	0.295	0.301	0.477
Ar	0.619	0.382	0.373	0.380	0.579
$\bar{\triangle}$	0.030	0.176	0.183	0.177	

are inadequate, the numbers are off by about 100%.

A similar picture is found for molecules. The KLICS highest occupied orbital energies listed in Table 4 for some diatomic molecules are in much better agreement with the experimental values than the conventional LDA and GGA schemes. We conclude that orbital energies are universally improved for atoms and molecules in the KLICS approach. This statement, however, is not true for molecular total energies as can be seen from the dissociation energies listed in Table 5.

Similar to Hartree-Fock, the dissociation energies of some molecules as calculated within the KLICS approximation are seriously in error. Since the corresponding *atomic* ground-state energies given above are of excellent quality, the error must be due to correlation effects

Table 4: *Energies of the highest occupied molecular orbitals of LiH, BH and FH from various calculations. The KLICS, PW91 and xcLDA results have been obtained with our basis-set-free numerical code at experimental bond lengths from [37]. The exact values of the ionization potential are from [37]. All numbers in atomic units.*

	KLICS	PW91	xcLDA	exact
LiH	-0.3224	-0.1623	-0.1613	-0.283
BH	-0.3698	-0.2052	-0.2031	-0.359
FH	-0.6772	-0.3577	-0.3608	-0.589

Table 5: *Dissociation energies of the closed-shell-first-row dimers calculated at experimental bond lengths from [37], except for HF, where the used bond lengths were 1.4 a.u. for H_2, 5.051 a.u. for Li_2, 4.6 a.u. for Be_2, 2.348 a.u. for C_2, 2.068 a.u for N_2 and 2.668 a.u. for F_2. Experimental values calculated from [37] by the method used in [38], except for H_2, where the exact value is from [39]. HF results calculated from values given in [40, 41]. All values calculated with basis-set free, fully numerical codes and given in 10^{-3} atomic units.*

	HF	KLICS	LDA	PW91	experiment
H_2	133.630	171.349	179.897	170.657	174.475
Li_2	17.0	32.4	37.9	33.4	39.3
Be_2	-12.3	-10.5	20.5	16.0	3.8
C_2	29.4	74.8	267.5	239.1	233.5
N_2	191.1	282.7	427.1	387.4	363.9
F_2	-45	-33	125	107	62.1

present in molecules only. In particular, the left-right correlation error, well known in HF theory, also occurs in DFT when the exact Fock expression for E_x is employed. Apparently this error is not sufficiently corrected for by the Colle-Salvetti funtional. The PW91 and LDA results are clearly much better. The fact that exchange effects are treated only approximately in these approaches seems to be an advantage. Therefore, the construction of correlation functionals better adapted to correct the left-right deficiency of the exact exchange energy functional is necessary. Work along these lines is in progress. A detailed study of x-only KLI results for molecules may be found in [32].

3.2 Solids

As pointed out in the previous sections, the OEP integral equation can be solved for spherically symmetric systems. This fact was exploited by Kotani [22, 23, 24], who implemented the exact exchange OEP into the tight-binding linear muffin-tin orbital method in the atomic sphere approximation (TB-LMTO-ASA) [42, 43, 44]. Starting point is the chain-rule relation

$$\frac{\delta E_{\mathrm{xc}}[\{\varphi\}]}{\delta V_S(\mathbf{r})} = \int \mathrm{d}^3 r' \underbrace{\frac{\delta E_{\mathrm{xc}}[\{\varphi\}]}{\delta \rho(\mathbf{r}')}}_{=V_{\mathrm{xc}}(\mathbf{r}')} \frac{\delta \rho(\mathbf{r}')}{\delta V_S(\mathbf{r})}. \tag{45}$$

Due to the spherical symmetry inside the atomic spheres within the ASA this integral equation can be solved numerically for the xc potential $V_{\mathrm{xc}}(\mathbf{r}')$. The functional derivatives with respect to the potential are calculated by differentiating E_{xc} and $\rho(\mathbf{r})$ with respect to the LMTO-parameters and the latter with respect to the potential.

Eq. (45) is equivalent to the OEP integral equation, which can easily be seen by applying the chain-rule of functional derivatives on the left-hand side of Eq. (45) leading to

$$\frac{\delta E_{\mathrm{xc}}[\{\varphi\}]}{\delta V_S(\mathbf{r})} = \sum_i \int \mathrm{d}^3 r' \frac{\delta E_{\mathrm{xc}}[\{\varphi\}]}{\delta \varphi_i(\mathbf{r}')} \frac{\delta \varphi_i(\mathbf{r}')}{\delta V_S(\mathbf{r})} + c.c. \tag{46}$$

where

$$\frac{\delta \varphi_i(\mathbf{r})}{\delta V_S(\mathbf{r}')} = G_{Si}(\mathbf{r}, \mathbf{r}') \varphi_i(\mathbf{r}), \tag{47}$$

with the KS Green's function G_{Si} defined in Eq. (33). The functional derivative of $\rho(\mathbf{r}')$ with respect to $V_S(\mathbf{r})$ can be identified with the KS response function

$$\frac{\delta \rho(\mathbf{r}')}{\delta V_S(\mathbf{r})} = \chi_S(\mathbf{r}', \mathbf{r}) = \sum_{i=1}^N G_{Si}(\mathbf{r}', \mathbf{r}) \varphi_i^*(\mathbf{r}') \varphi_i(\mathbf{r}) + c.c.. \tag{48}$$

Inserting (46) and (47) on the left-hand side and (48) on the right-hand side of Eq. (45) and using the definition of the $u_{\mathrm{xc}i}(\mathbf{r})$, Eq. (32), one recovers the OEP integral equation (31).

Kotani added an LDA correlation energy functional, using the von Barth-Hedin parametrization, and applied this method (EXX, for exact exchange) to insulators [22], semiconductors [23] and most recently to metals [24]. Some results for insulators and semiconductors are given in Tables 6 and 7. The energies found for metals are in good agreement with LDA results.

Another approach was devised by Bylander and Kleinman [45]. They implemented the KLI approximation within a pseudo-potential framework. As in the previous method, correlation effects were taken into account through an ordinary LDA, which was added to the KLI exchange-potential. The results for Ge are given in Table 7.

Table 6 shows the results of the EXX method for MgO and CaO. The values of the gap obtained with this method lie inbetween the LDA and the HF results and are in much better agreement with the experimental values. It has to be noted that the derivative discontinuities, which can in principle be calculated with the EXX method, are not taken

Table 6: *Energy gaps (in eV) at high-symmetry points for MgO and CaO from Ref. [22]*

		LDA	EXX	APW-LDA	Hartree-Fock	experiment
MgO	Direct Gap					
	Γ	4.64	6.21	4.7	25.3	7.833
	X	13.56	15.23	10.2	17.0	
	L	12.91	14.33	8.3	21.4	
CaO	Direct Gap					
	Γ	4.30	6.47	4.4	15.8	7.09
	X	4.30	7.40	3.9	19.9	
	L	7.78	10.12	7.9	21.9	
	Indirect Gap					
	$\Gamma - X$	3.96	6.97	3.5	18.7	

into account here. The width of the oxygen $(2p)$ states is reduced with respect to an LDA-calculation, which is caused by the self-interaction cancellation of the EXX method making these states more localized. Furthermore the potential within the atomic spheres displays more structure than the corresponding LDA potential [22]. This is analogous to the inter-shell peaks discussed above for atoms.

In Table 7 the results for Si, Ge and diamond are compared for various schemes, respectively. All energies are relative to the top of the valence band which, in these systems, is the $\Gamma_{25'}$ state. Compared with the LDA results, the energies of the conduction band are consistently shifted upwards, i.e. towards the HF values, by the OEP method. As before, the overall agreement with experiment is much better in the OEP schemes than in LDA or HF. Once again, the discontinuity of the xc potential, although it can be calculated within the OEP method, was *not* taken into account in these calculations.

The importance of this discontinuity was estimated by Li, Krieger, Norman and Iafrate [47], who applied the OEP and the KLI approximately to a Perdew-Zunger SIC-LDA. Results for the energy gaps of noble-gas solids and NaCl are given in Table 8. It is clearly visible that the values of $(E_{KS}^g + \Delta_{xc})$ are in much better agreement with experiment than the mere KS gaps.

Table 7: *Comparison of the KS-eigenvalues (in eV) relative to the top of the valence band ($\Gamma_{25v'}$) for Si, Ge and diamond. The LDA, EXX and also the experimental values are taken from Ref. [23]. HF values are from Ref. [46]. KLI values are from Ref. [45].*

		LDA	EXX	HF	KLI	experiment
Si	gap	0.45	1.93			1.17
	Γ_{15c}	2.65	3.79	8.7		3.4
	$\Gamma_{2c'}$	3.07	4.43	9.3		4.2
	L_{1c}	1.41	2.65			2.1, 2.4 $\pm$ 0.15
	L_{3c}	3.22	4.31			4.15 $\pm$ 0.1
	Γ_{1v}	-12.07	-11.35			-12.5 $\pm$ 0.6
	X_{4v}	-2.92	-2.46			-2.9, -3.3 $\pm$ 0.2
	$L_{3v'}$	-1.20	-0.91			-1.2 $\pm$ 0.2, 1.5
Ge	Γ_{15c}	2.70	3.55	7.9		3.24
	$\Gamma_{2c'}$	0.40, -0.20[a]	1.90	4.3	1.239	0.98
	$L_{1c}(gap)$	0.32	1.57		0.796	0.87, 0.84[b]
	L_{3c}	3.67	4.43			4.3
	X_{1c}	0.630			0.933	1.3 $\pm$ 0.2[b]
	Γ_{1v}	-12.68	-12.01			-12.6 $\pm$ 0.3
	L_{1v}	-7.62	-6.99			-7.7 $\pm$ 0.2, -7.4 $\pm$0.2
	$L_{3v'}$	-1.40	-1.15			-1.4 $\pm$ 0.2
diamond	gap	4.00	5.12			5.48
	Γ_{15c}	5.61, 5.7[c]	6.61	14.6		7.3
	$\Gamma_{2c'}$	13.50,13.4[c]	14.04	23.7		15.3 $\pm$ 0.5
	Γ_{1v}	-21.6	-21.4			-24.2 $\pm$ 1, -21 $\pm$ 1
	L_{1v}	-13.65	-13.09			-12.8 $\pm$ 0.3

[a] *conventional LDA in TB-LMTO-ASA from [46]*

[b] *values are taken from [45]*

[c] *conventional LDA-pseudopotential calculation from [45]*

Table 8: *Gap energies (in eV) of noble-gas solids and NaCl. The values in parentheses are calculated without the derivative discontinuity (from Ref. [47]).*

	LDA	OEP $E^g(E^g_{\mathrm{KS}})$	KLI $E^g(E^g_{\mathrm{KS}})$	SIC	experiment
Ne	11.5	20.9 (15.2)	20.8 (15.2)	22.2	21.4
Ar	8.2	13.1 (9.7)	13.1 (9.7)	15.2	14.2
Kr	6.8	11.1 (8.0)	10.8 (7.9)	13.6	11.6
Xe	5.8	9.5 (6.9)	9.0 (6.7)		9.8
NaCl	5.5	9.5 (6.3)	9.5 (6.4)	10.0	9.0

4   Acknowledgments

References

[1] R.T. Sharp and G.K. Horton, Phys. Rev. **90**, 317 (1953).

[2] P. Hohenberg and W. Kohn, Phys. Rev. **136**, B864 (1964).

[3] Q. Zhao and R.G. Parr, Phys. Rev. A **46**, 2337 (1992).

[4] C.J. Umrigar and X. Gonze, in *High Performance Computing and its Application to the Physical Sciences*, edited by D.A. Browne et al (World Scientific, Singapore, 1993).

[5] C.J. Umrigar and X. Gonze, Phys. Rev. A **50**, 3827 (1994).

[6] R. van Leeuven and E.J. Baerends, Phys. Rev. A **49**, 2421 (1994).

[7] A. Görling and M. Ernzerhof, Phys. Rev. A **51**, 4501 (1995).

[8] V.E. Ingamells and N.C. Handy, Chem. Phys. Lett. **248**, 373 (1996).

[9] W. Kohn and L.J. Sham, Phys. Rev. **140**, A1133 (1965).

[10] J.B. Krieger, Y. Li, and G.J. Iafrate, Phys. Rev. A **45**, 101 (1992).

[11] J.B. Krieger, Y. Li, and G.J. Iafrate, in *Density Functional Theory*, edited by R.M. Dreizler and E.K.U. Gross (Plenum Press, New York, 1995).

[12] C.A. Ullrich, U.J. Gossmann, and E.K.U. Gross, Phys. Rev. Lett. **74**, 872 (1995).

[13] C.A. Ullrich, S. Erhard, and E.K.U. Gross, in *Superintense Laser Atom Physics IV*, edited by H.G. Muller (Kluwer, Dordrecht, 1996).

[14] M. Petersilka, U.J. Gossmann, and E.K.U Gross, Phys. Rev. Lett. **76**, 1212 (1996).

[15] E.K.U. Gross, J.F. Dobson, and M. Petersilka, in *Topics in Current Chemistry*, edited by R.F. Nalewajski (Springer, Berlin, 1996).

[16] U. von Barth and L. Hedin, J. Phys. C **5**, 1629 (1972).

[17] M.M. Pant and A.K. Rajagopal, Sol. State Commun. **10**, 1157 (1972).

[18] A. Görling and M. Levy, Phys. Rev. A **50**, 196 (1994).

[19] J.D. Talman and W.F. Shadwick, Phys. Rev. A **14**, 36 (1976).

[20] T. Grabo and E.K.U. Gross, Chem. Phys. Lett. **240**, 141 (1995).

[21] E. Engel and S.H. Vosko, Phys. Rev. A **47**, 2800 (1993).

[22] T. Kotani, Phys. Rev. B **50**, 14816 (1994), and Erratum (submitted).

[23] T. Kotani, Phys. Rev. Lett. **74**, 2989 (1995).

[24] T. Kotani and H. Akai, Phys. Rev. B **52**, 17153 (1995).

[25] Y. Li, J.B. Krieger, and G.J. Iafrate, Phys. Rev. A **47**, 165 (1993).

[26] R.M. Dreizler and E.K.U. Gross, *Density Functional Theory* (Springer, Berlin, 1990).

[27] A.D. Becke, Phys. Rev. A **38**, 3098 (1988).

[28] J.P. Perdew, K. Burke, and Y. Wang, Phys. Rev. B (1996), (submitted).

[29] J.A. Montgomery, J.W. Ochterski, and G.A. Petersson, J. Chem. Phys. **101**, 5900 (1994).

[30] E.R. Davidson, S.A. Hagstrom, S.J. Chakravorty, V.M. Umar, and C. Froese Fischer, Phys. Rev. A **44**, 7071 (1991).

[31] A.A. Radzig and B.M. Smirnov, *Reference Data on Atoms and Molecules* (Springer, Berlin, 1985).

[32] T. Grabo and E.K.U. Gross, Int. J. Quantum Chem. (1996), in press.

[33] E.K.U. Gross, M. Petersilka, and T. Grabo, in *Chemical Applications of Density Functional Theory, ACS Symposium Series 629*, edited by B.B Laird, R.B. Ross, and T. Ziegler (American Chemical Society, Washington, DC, 1996).

[34] R. Colle and D. Salvetti, Theoret. Chim. Acta **37**, 329 (1975).

[35] R. Colle and D. Salvetti, Theoret. Chim. Acta **53**, 55 (1979).

[36] C. Lee, W. Yang, and R.G. Parr, Phys. Rev. B **37**, 785 (1988).

[37] K.P. Huber and G. Herzberg, *Molecular Spectra and Molecular Structure: IV. Constants of Diatomic Molecules* (Van Nostrand Reinhold, New York, 1979).

[38] C. Filippi and C.J. Umrigar, J. Chem. Phys. **105**, 213 (1996).

[39] W. Kolos and L. Wolniewicz, J. Chem. Phys. **49**, 404 (1968).

[40] L. Laaksonen, P. Pyykkö, and D. Sundholm, Comp. Phys. Reports **4**, 313 (1986).

[41] C. Froese Fischer, *The Hartree-Fock method for atoms* (Wiley, New York, 1977).

[42] O. K. Andersen, O. Jepsen, and D. Glötzel, in *Highlights of Condensed-Matter Theory*, edited by F. Bassani, F. Fumi, and M. P. Tosi (North-Holland, Amsterdam, 1985), p. 59.

[43] O. K. Andersen, Z. Pawloska, and O. Jepsen, Phys. Rev. B **34**, 5253 (1986).

[44] H. L. Skriver, *The LMTO method* (Springer, New York, 1984).

[45] D. M. Bylander and L. Kleinman, Phys. Rev. Lett. **74**, 3660 (1995).

[46] A. Svane, Phys. Rev. B **35**, 5496 (1987).

[47] Y. Li, J. B. Krieger, M. R. Norman, and G. J. Iafrate, Phys. Rev. B **44**, 10437 (1991).